

PACS numbers: 42.81.Cn; 42.81.Dp
DOI: 10.1070/QE2003v033n07ABEH002470

Mechanisms of optical losses in fibres with a high concentration of germanium dioxide

M.E. Likhachev, M.M. Bubnov, S.L. Semenov,
V.V. Shvetsov, V.F. Khopin, A.N. Gur'yanov, E.M. Dianov

***Abstract*. The mechanisms of optical losses determining the scattering of light in single-mode fibres with a high germanium-dioxide content in a core are investigated. The coefficients of the Rayleigh scattering in fibres with a high level of doping (a molar concentration of GeO_2 of up to 30 %) are measured for the first time. The investigations of the angular distribution of the intensity of light scattered from the fibre have revealed the presence of an additional, anomalous scattering of light besides the Rayleigh scattering. The nature of this phenomenon is discussed.**

Keywords: *fibre optics, highly doped fibres, germanosilicate fibre, optical losses, light scattering, Rayleigh scattering.*

1. Introduction

Single-mode fibres employed in communication systems commonly have a relatively low level of doping by germanium dioxide (a molar concentration of 3 % – 10 %). Optical losses in these fibres are 0.18 – 0.22 dB km^{-1} (at a wavelength of 1.55 μm) and are close to a theoretical limit, which is determined by three fundamental mechanisms: Rayleigh scattering, phonon and electron absorption.

The increase in the molar concentration of germanium dioxide in the fibre core to 20 % – 30 % leads to the enhancement of the nonlinear properties of fibres due to both the increase in the nonlinearity factor of highly doped fused silica and the significant rise of the light intensity in the core because of the decrease in the mode-field diameter. Such fibres are of undoubted interest for the development of a diversity of nonlinear fibre devices, for example, Raman lasers and amplifiers, parametric amplifiers, and nonlinear switches [1 – 4]. Optical losses in the fibres substantially affect the efficiency of these devices. However, for the doping level required for the creation of efficient nonlinear devices (the molar concentration of GeO_2 of 24 % – 30 %), the level of optical losses in best single-mode fibres, produced by the MCVD technique, is at present respectively 0.8 – 3.0 dB km^{-1} ($\lambda = 1.55$ μm) [1, 5, 6], which is significantly higher than the level of losses determined by fundamental mechanisms.

Many papers were devoted to the elucidation of the origin of 'excess' losses in highly doped single-mode fibres. The increase in optical losses was explained, for example, by the appearance of an additional absorption caused by stressed or dissociated bonds at the core – cladding interface in the fibre, which resulted from the difference in the coefficients of thermal expansion of the core and cladding materials [7 – 9]. Some authors explained high optical losses by strong Rayleigh scattering. This assumption was based on the fact that spectral dependences of 'excess' optical losses in the fibre are similar to those of losses caused by Rayleigh scattering [10, 11]. The possibility of the induction of optical losses in the process of drawing by UV radiation from the heating area of the furnace was studied [12, 13]. In recently published works [14, 15], the anomalous scattering, whose intensity unlike that of the Rayleigh scattering is considerable at small angles with the fibre axis, was observed.

Nevertheless, the convincing experimental evidence of one or another mechanism of losses has not been obtained so far. Moreover, the authors of paper [16] pointed out that the scattering losses dominate in the visible and near-IR regions. This fact allows one if not to reject mechanisms explaining the excess losses by the increase in absorption, then at least to relate them to secondary. Furthermore, the investigations performed by different research groups have demonstrated that optical losses in highly doped fibres depend on a number of technological factors such as the drawing temperature, fibre tension during drawing, shape of the core refractive-index profile, composition of the core and cladding of the fibre. In particular, the additional codoping of the fibre core with fluorine and reduction of the drawing temperature reduced the level of optical losses [7, 17, 18].

The aim of this work is to study mechanisms related to Rayleigh and anomalous scattering. For this purpose, the Rayleigh scattering coefficients have been determined within a wide range of GeO_2 concentrations. The dependences of the anomalous scattering on the shape of the refractive-index profile and temperature of the fibre drawing have been studied to ascertain the mechanisms of this scattering.

M.E. Likhachev, M.M. Bubnov, S.L. Semenov, V.V. Shvetsov, E.M. Dianov Fiber Optics Research Center, A.M. Prokhorov General Physics Institute, Russian Academy of Sciences, ul. Vavilova 38, 119991 Moscow, Russia;
V.F. Khopin, A.N. Gur'yanov Institute of Chemistry of High-Purity Materials, Russian Academy of Sciences, ul. Tropinina 49, 603950 Nizhnii Novgorod, Russia

Received 11 December 2002
Kvantovaya Elektronika **33** (7) 633 – 638 (2003)
Translated by Yu.M. Mikhailova

2. Fabrication of fibres with a high concentration of germanium dioxide

The fibre preforms were prepared by the MCVD technique using fused silica substrate tubes. The composition of the light reflecting cladding was $F-P_2O_5-SiO_2$ with the refractive index lower than that of fused silica by $(0.1-2)\times10^{-3}$. The core composition was $F-GeO_2-SiO_2$, the maximum molar concentration of germanium dioxide varied within the range of 14 % – 30 % (the relative refractive index difference between the core and the cladding $\Delta=\Delta n/n_{SiO_2}=1.24\,\%-2.9\,\%$). To reduce optical losses, freon-113 ($C_2F_3Cl_3$) was injected into the gas mixture during the deposition of layers [18]. The absorption peak corresponding to OH groups did not exceed 1 dB km^{-1} at a wavelength of 1.39 μm. To reveal the influence of the drawing conditions on optical losses, the fibres were drawn at different temperatures of the furnace.

3. Investigation of Rayleigh scattering

To determine the Rayleigh scattering coefficients in the fibre, most authors [1, 10, 11, 18, 19] use the so-called λ^{-4} analysis: the spectrum of optical losses $\alpha(\lambda)$ in the fibre is plotted in λ^{-4} coordinates and the spectral region, where the fibre works in a single-mode regime, is approximated by a straight line. From the line slope one can find a phenomenological Rayleigh scattering coefficient A:

$$\alpha(\lambda)=\frac{A}{\lambda^4}+B. \tag{1}$$

Here, the coefficient B determines the level of the so-called imperfection losses, which are independent of the wavelength. However, the λ^{-4} technique has its own limitations, since all optical losses depending on the wavelength are taken into account when determining the Rayleigh scattering coefficient, and if besides the Rayleigh scattering another spectral-selective mechanism of optical losses is present, the coefficient A obtained by the λ^{-4} analysis may appreciably differ from the actual Rayleigh scattering coefficient.

In this work, the Rayleigh scattering coefficients in fibres with different GeO_2 concentrations were measured by the OTDR technique [20]. In this technique the short laser pulse is coupled into the fibre, being partially scattered and partially absorbed during the propagation through the fibre. A part of the scattered radiation passes through the fibre in the direction opposite to the probe pulse propagation direction and is detected by a photodetector. The power of detected light is

$$P=P_0\eta(z_0)\exp\left(-2\int_0^{z_0}\gamma(z)\mathrm{d}z\right), \tag{2}$$

where P_0 is the power of radiation coupled into the fibre; $\gamma(z)$ is the coefficient of the light attenuation in the fibre; η is the backscattering coefficient; and z_0 is the coordinate of the point at which the light was scattered.

Assuming that the backward scattering of light is the result of Rayleigh scattering (we will see in Section 4 that this is reasonable) and considering the mode-field distribution over the radius to be Gaussian, we can deduce the relation between the backscattering coefficient η and the local coefficient of Rayleigh scattering α_{Rel} [21]:

$$\eta(z)\propto\frac{\tau v}{\lambda^2 n^2}\frac{\alpha_{Rel}(z)}{w^2(z)}, \tag{3}$$

where τ is the pulse duration; v is the group velocity; n is the refractive index of the fibre core; w is the mode-field diameter; and λ is the wavelength.

The ratio of the Rayleigh scattering coefficients of any two fibres can be obtained in the following way (Fig. 1). Two fibres under study are spliced or joined through the mechanical junction, and the backscattering signals from the two free ends of joined fibres are measured. At the junction of the fibres, the backscattering signal changes sharply because of the difference of the backscattering coefficients η in the fibres and the decrease in the radiation power propagating though the fibre due to the attenuation γ_{12} introduced at the junction:

$$R_{12}=\frac{P_{12}}{P_{11}}=\frac{\eta_2}{\eta_1}\exp(-2\gamma_{12}), \tag{4}$$

$$R_{21}=\frac{P_{22}}{P_{21}}=\frac{\eta_1}{\eta_2}\exp(-2\gamma_{12}). \tag{5}$$

By using expressions (2) – (4), we obtain

$$\frac{\alpha_{Rel1}}{\alpha_{Rel2}}=\left(\frac{R_{21}}{R_{12}}\right)^{1/2}\left(\frac{n_1}{n_2}\right)^3\left(\frac{w_1}{w_2}\right)^2. \tag{6}$$

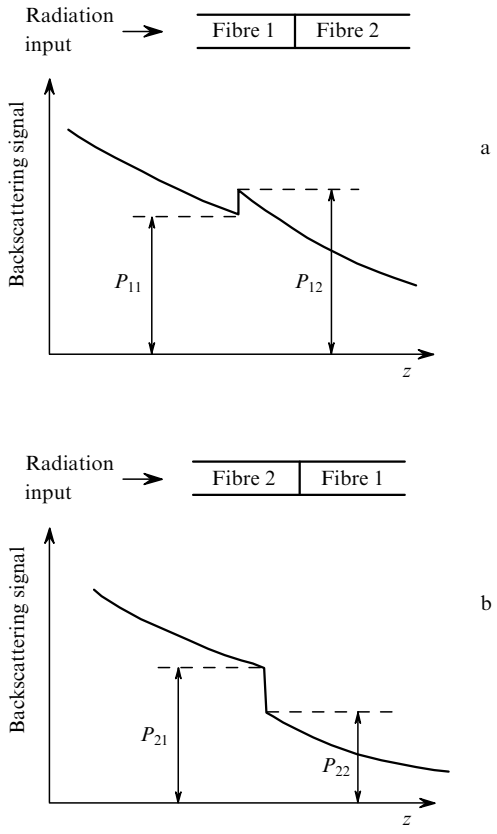

Figure 1. Schemes for measuring the ratio between the Rayleigh scattering coefficients in fibres 1 and 2 (a), as well as 2 and 1 (b) by means of the OTDR technique, and the dependences of the idealised backscattering signal on the coordinate z of the scattering point.

Expression (6) allows us to determine the ratio of the Rayleigh scattering coefficients of two fibres by measuring the backscattering signal jumps, mode-field diameters, and refractive index differences of both fibres. The absolute value of the Rayleigh scattering coefficient can be found by performing measurements using an 'etalon' fibre, i.e., the fibre in which the Rayleigh scattering coefficient is predetermined. In this work, a single-mode fibre with a silica core was used as such an etalon. The Rayleigh scattering coefficient in this fibre was assumed equal to the coefficient of the Rayleigh scattering in fused silica [22]. The measurements were performed at a wavelength of 1.31 μm, near the cutoff wavelength (~ 1.0 μm) of fibres under study.

The results of measurements of the Rayleigh scattering coefficients in fibres with the GeO_2 molar concentration of 14 % – 30 % are demonstrated in Fig. 2. The measurement error was determined by the error of measurements of the mode-field diameter and value of the stepwise change of the power at the junction and was equal to 10 %. A good agreement can be seen between our results and the results obtained by other authors in bulk samples and multimode fibres [19, 23] as well as the results of work [24], in which the backscattering technique also was used to measure the Rayleigh scattering coefficients in fibres with $\Delta = 0 - 11$ % and one fibre with $\Delta = 2.3$ %. At the same time, it follows from Fig. 2 that the Rayleigh scattering coefficients obtained by the λ^{-4} analysis from the spectra of optical losses of the fibres turned out to be substantially higher, because the λ^{-4} analysis takes into account not only losses due to the Rayleigh scattering but also other optical losses depending on the wavelength. Hence, a substantial difference between the results of the backscattering technique and λ^{-4}-analysis emerges, thus making the latter technique inapplicable for determining the Rayleigh scattering coefficients of single-mode fibres with high GeO_2 content (molar concentration greater than 10 %).

Linear approximation of the results we obtained (Fig. 2) allows us to find an analytic dependence of the Rayleigh scattering coefficients α_{Rel} on the relative difference between refractive indices of the core and cladding of the fibre Δ:

$$\alpha_{Rel} = 0.75(1 + 0.49\Delta)\ [\text{dB km}^{-1}\ \mu\text{m}^4]. \quad (7)$$

Expression (7) can be used to estimate the contribution of the Rayleigh scattering to optical losses of the single-mode fibre at the 1.55-μm wavelength. For the fibre with $\Delta = 3$ %, this contribution is equal to 0.33 dB km^{-1}. Thus, the increase in optical losses to 3 dB km^{-1} for single-mode fibres with the molar concentration of germanium dioxide in the core ~ 30 % cannot be explained only by the increase in Rayleigh scattering losses.

4. Anomalous scattering of light

The anomalous scattering of light in single-mode fibres was observed in papers [14, 15, 25]. The scattering intensity was significant only at small angles with the fibre axis, but the maximum intensity of the anomalous scattering substantially exceeded the Rayleigh scattering intensity. Only in one of these works [25], wherein fibres with low germanium-dioxide content were investigated, the distribution of the intensity of light scattered at small (less than 10°) angles was measured. In the rest two papers only the 'tail' of the anomalous scattering was recorded.

To study the scattering of this type, we constructed an experimental setup for measuring the intensity of scattered light within the range of angles of 1 – 16° with the fibre axis (Fig. 3), both in the probe radiation propagation direction (scheme *1*) and in the opposite direction (scheme *2*). A part of the fibre under study without the polymer coating was placed into a tank with an immersion liquid. The refractive index of the immersion liquid was slightly higher than the fused silica refractive index, thus allowing for the coupling almost all scattered radiation out the fibre. The critical angle was 2°. Radiation of a Nd : YAG laser at 1.06-μm was coupled into the one end of the fibre. Radiation scattered at a certain angle with the fibre was reflected from the mirror and converged to a point in the focal plane of the lens. The distribution of the light intensity as a function of the scattering angle in the fibre cladding was calculated from the measured distribution of light in the focal plane of the lens. The results of measurements were averaged over three–four different segments of the fibre.

Fig. 4 shows the results of measurements of the intensity of light scattered in the fibre with the GeO_2 molar

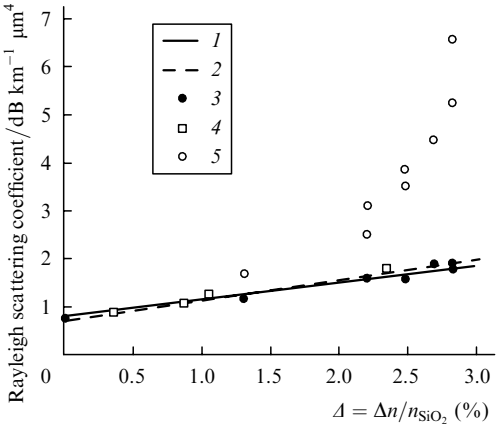

Figure 2. Rayleigh scattering coefficients versus the level of doping by germanium dioxide: (*1*) bulk samples, approximation of measurements for $\Delta = 0 - 1$ % [23]; (*2*) multimode fibres, λ^{-4}-analysis [19]; (*3*) single-mode fibres, OTDR technique (the present work); (*4*) single-mode fibres, OTDR technique [24]; (*5*) single-mode fibres, λ^{-4}-analysis (the present work).

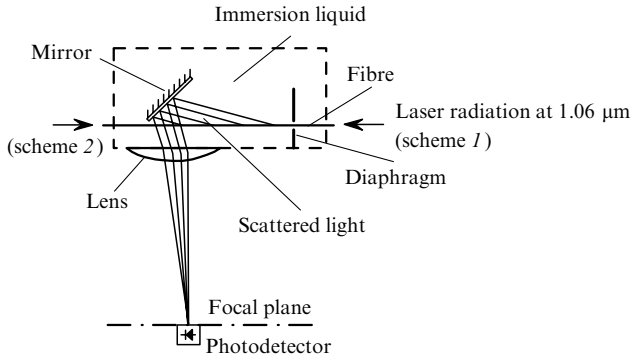

Figure 3. Experimental setup for measuring the intensity of light scattered at small angles.

concentration of 27 % ($\Delta = 2.6$ %). Curve (*1*) represents the angular dependence of the intensity of light scattered in the direction of the probe radiation propagation [radiation was coupled into fibres using scheme (*1*)]. Curve (*2*) corresponds to the intensity of light scattered in the opposite direction [radiation was coupled into fibres using scheme (*2*)]. The presented results demonstrate that the light scattering differs from Rayleigh scattering, and instead of the dependence $I_0(1 + \cos\theta)$ an absolutely different angular distribution is observed. The scattering indicatrix is assymmetric: the power scattered in the direction of light propagation is significantly greater than that scattered in the backward direction. Moreover, the clearly pronounced maxima of the power at small angles with the fibre axis are observed. Thus, optical losses in the fibre are caused by one more kind of scattering besides the Rayleigh one. Further, this kind of scattering will be called near-forward [25]. Note that the intensity of the near-forward scattering sharply decreases at angles of propagation in the cladding tending to zero. This fact justifies the assumption, made in Section 3, that the backscattering trapped by the fibre core is mainly Rayleigh scattering.

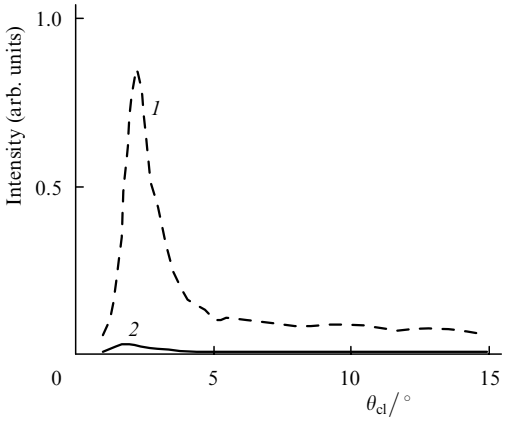

Figure 4. Angular dependences of the intensity of scattered light in the direction of the radiation propagation (*1*) and in the backward direction (*2*).

To study the main factors influencing the distribution of the intensity of the near-forward scattering, two preforms with gradient and step refractive index profiles (RIPs) and approximately equal doping levels (the GeO_2 molar concentration ~ 27 %) were fabricated. The fibres were drawn of these preforms at two different temperatures of the furnace. It is well known that the reduction of the drawing temperature leads to the decrease in optical losses of fibres [7, 17]. The results presented in Fig. 5 show that the reduction of the drawing temperature results also in the substantial decrease in the near-forward scattering; simultaneously, the shift of its maximum is observed. The comparison of optical characteristics of two fibres possessing different RIPs and drawn at the same temperature (Fig. 6) demonstrates that the gradient form of the RIP of the core leads to the noticeable decrease in both total optical losses in the fibre and the near-forward scattering intensity. The difference in intensities of the near-forward scattering in 'tails' of the distributions, which, in fact, make the main contribution to the total scattered power, is especially noticeable.

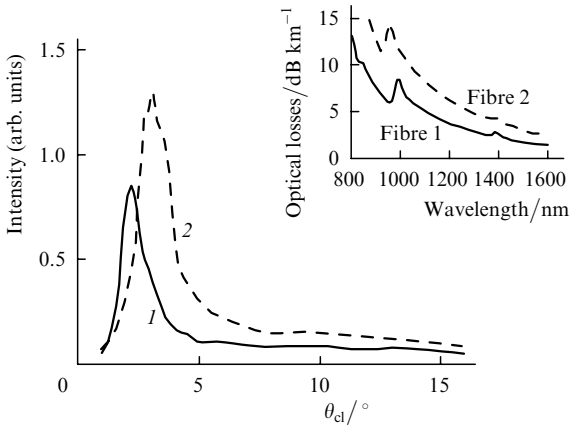

Figure 5. Angular dependences of the scattered light intensity in the fibre cladding (angles are counted from the radiation propagation direction) for low (*1*) and high (*2*) temperatures of drawing of the fibre with the gradient refractive index profile; $\Delta = 2.6$ %. The inset displays spectra of optical losses in fibres 1 and 2.

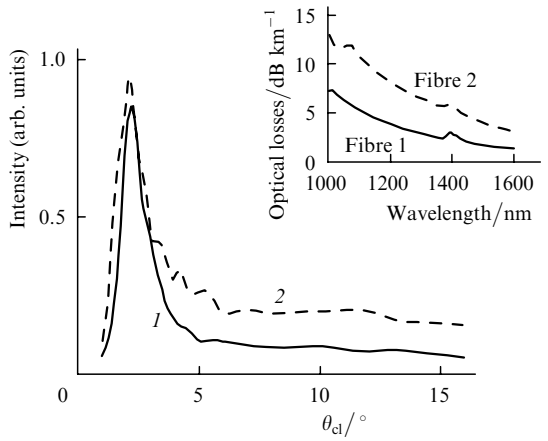

Figure 6. Angular dependences of the scattered light intensity in the fibre cladding (angles are counted from the radiation propagation direction) for the gradient (*1*) and step-index (*2*) fibres; $\Delta = 2.6$ %. The inset displays spectra of optical losses in fibres 1 and 2.

The results of measurements presented in Fig. 4 allow the preliminary estimation of the contribution of near-forward scattering to total fibre losses. Our estimates were based on the assumption that the scattering in the opposite direction to the probe radiation propagation [curve (*2*), Fig. 4] at angles greater than 10° is Rayleigh scattering. The coefficient of Rayleigh scattering was determined from the results of measurements described in Section 3. This allowed us to normalise the intensity of the near-forward scattering and to determine the absolute value of near-forward scattering losses by calculating the power of light scattered from the known length of the fibre,

$$P_{sc} = \int_0^{16^\circ} 2\pi I \sin\theta \mathrm{d}\theta. \qquad (8)$$

We found that the near-forward scattering at 1.06-μm in the fibre with $\Delta = 2.6$ % (see Fig. 4) was no less than 1.6 dB× km^{-1}, while total losses were 6 dB km^{-1} and Rayleigh

scattering losses were 1.2 dB km^{-1}. This estimate is the lower estimate because the measurements of the near-forward scattering were limited by the range of angles lower than 16°, and the contribution of the neglected part of the near-forward scattering (at angles greater than 16°) can be significant.

Unfortunately, we did not succeed in measuring the near-forward scattering in the range of wavelengths greater than 1.2 μm because of the significant absorption of the immersion liquid in this range. However, it is known that total losses are approximated with high accuracy by a straight line in coordinates λ^{-4} [1, 10, 18], while Rayleigh scattering depends on the wavelength as λ^{-4}, therefore it can be assumed that the near-forward scattering has the wavelength dependence also close to λ^{-4}. The theoretical analysis of possible mechanisms determining the near-forward scattering [26, 27] also yields the dependence close to $\lambda^{-3} - \lambda^{-4}$.

5. Discussion

Our investigations have demonstrated that in fibres with a high concentration of germanium dioxide ($\Delta = 2\,\% - 3\,\%$) optical losses caused by the Rayleigh scattering do not exceed 0.33 dB km^{-1}. Contributions of the electron and phonon absorption to optical losses of the fibre with the GeO_2 molar concentration of 27 % at a 1.55-μm wavelength are 0.07 and 0.02 dB km^{-1}, respectively [19]. Thus, the presence of high optical losses (greater than 1 – 3 dB km^{-1}) in the fibres doped by GeO_2 with molar concentration of 25 % – 30 % is explained only by the existence of other loss mechanisms. According to our study, significant losses can arise from the near-forward scattering, the properties of which differ from those of Rayleigh scattering and whose nature is not completely clear.

By the present time, the two mechanisms have been proposed to explain the near-forward scattering. The first of them considered by Marcuse [26] and Rawson [27] presumes the light scattering by the variations of the dimensions and form of the core – cladding interface along the fibre length. The theoretical analysis performed by these authors has shown that in this case the light scattering would have the near-forward character, i.e., the intensity of the scattered light would have maximum at the small angle with the fibre axis and sharply decrease at greater angles of scattering. The second mechanism proposed by Rawson [25] describes the light scattering by needle-shaped inhomogeneities parallel to the fibre axis, which can arise in the drawing process, for example, as a result of tapering the micro-areas with the increased GeO_2 concentration, which appear, in the opinion of authors of Ref. [6], in the bulk of the highly doped preform in the process of its fabrication. The theoretical analysis has shown that in this case too, the maximum of the intensity of scattered light will be observed at a small angle with the fibre axis [25].

The experimental data available at present allow one to reject the second mechanism of the origin of the near-forward scattering. First, our investigations have demonstrated that its intensity depends on the form of the refractive index profile (it decreases when using the gradient RIP instead of the step). The fibres with different RIPs were fabricated with the identical technique; they had close concentrations of germanium dioxide and, to all appearance, identical quantities of micro-inhomogeneities in the bulk of the preform. Therefore, if the second mechanism of the near-forward scattering, namely, the scattering by needle-shaped inhomogeneities, was valid, a significant change in the near-forward scattering intensity would not be observed. Second, the dependence of the intensity of the near-forward scattering on the fibre drawing temperature testifies against the scattering by needle-shaped inhomogeneities. As is demonstrated by Rawson's calculations [25], the intensity of the near-forward scattering is proportional to the wavelength of scattered light, dimensions of 'needles', average value of the inhomogeneity produced by these needles (Δn is implied) and density of distribution of 'needles' in the bulk of the fibre. When the fibre drawing temperature is reduced, all these parameters practically do not change, however the intensity of the near-forward scattering significantly decreases (see Section 4 and Fig. 5).

In our opinion, the near-forward scattering is most probably caused by the variations of the core – cladding interface in the fibre along the fibre length. When tapering the preform with the step RIP, a jump of viscosity at the core – cladding interface, which can lead to the variations of the interface between different glasses, appears in the fibre-forming zone. As the drawing temperature decreases, the viscosity of glasses in the fibre-forming zone rises, as a result of which the amplitude of the variations and, consequently, the near-forward scattering, related to it, should decrease. This very effect was observed in our experiments. In case of tapering the preforms with the gradient RIP, a sharp jump of the viscosity in the fibre-forming zone does not appear, therefore the variations of the core – cladding interface become smaller. It should be noted that the increase in the core-doping level leads to the rise of the difference of coefficients of thermal expansion of the core and cladding glasses of the fibre. As a result, when cooling the fibre from the drawing temperature to the room temperature, the stresses appear at the core – cladding interface. These stresses can deform the fibre core, which also leads to the variations of the core – cladding interface along the fibre length.

6. Conclusions

Investigations of optical losses caused by the light scattering in highly doped (the molar concentration of GeO_2 of 24 % – 30 %) fibres, fabricated by the MCVD technique, have been performed. These investigations have demonstrated that with the rise of the germanium dioxide concentration the Rayleigh scattering coefficient increases linearly within the limits of error. This result is in a good agreement with the data for multimode fibres and bulk samples. The contribution of Rayleigh scattering to optical losses does not exceed 0.35 dB km^{-1} for $\Delta < 3\,\%$. We have ascertained that the considerable increase in optical losses, occurring at high GeO_2 concentrations in single-mode fibres, is caused by an additional loss mechanism – the near-forward scattering, which results, in our opinion, from the variations of the core – cladding interface along the fibre length.

Acknowledgements. The authors thank the group of I.A. Bufetov and especially to A.V. Shubin for performing the measurements of the mode-field size, as well as K.M. Golant for the fibre with the pure silica core placed at our disposal. The authors are grateful to O.N. Egorova

for her significant contribution to the construction of the experimental setup for measuring the near-forward scattering.

References

1. Davey S.T., Williams D.L., Spirit D.M., Ainslie B.J. *Proc. SPIE Int. Soc. Opt. Eng.*, **1171**, 181 (1989).
2. Dianov E.M., Abramov A.A., Bubnov M.M., Prokhorov A.M., Shipulin A.V., Devjatykh G.G., Guryanov A.N., Khopin V.F. *Electron. Lett.*, **31** (13), 1057 (1995).
3. Dianov E.M., Bufetov I.A., Bubnov M.M., Grekov M.V., Vasiliev S.A., Medvedkov O.I., Shubin A.V., Guryanov A.N., Khopin V.F., Yashkov M.V., DeLiso E.M., Butler D.L. *Proc. SPIE Int. Soc. Opt. Eng.*, **4083**, 101 (2000).
4. Pastel D.A., Evans A.F., Hawk R.M., Nolan D.A., Weidman D.L., Dasika P., Jiang M., Islam M.N., Moodie D.G. *OFC'97 Tech. Dig.* (Dallas, Texas, 1997) WL6b, p. 168.
5. Abramov A.A., Bubnov M.M., Dianov E.M., Golant K.M., Khrapko R.R., Semjonov S.L., Shebunjaev A.G., Gurjanov A.N., Khopin V.F. *OFC'95 Tech. Dig.* (San Diego, California, 1995) WP4, p. 173.
6. Dianov E.M., Mashinsky V.M., Neustruev V.B., Sazhin O.D., Guryanov A.N., Khopin V.F., Vechkanov N.N. *Opt. Fiber Techn.*, **3**, 77 (1997).
7. Ainslie B.J., Beales K.J., Day C.R., Rush J.D. *IEEE J. Quantum Electron.*, **17**, 854 (1981).
8. Ainslie B.J., Beales K.J., Cooper D.M., Day C.R., Rush J.D. *J. of Non-Cryst. Solids*, **47**, 243 (1982).
9. Kajioka H., Kumagai T., Ishikawa T., Teraoka T. *OFC'88* (New Orleans, Louisiana, 1988) WI3, p. 75.
10. Sudo S., Itoh H. *Opt. Quantum Electron.*, **22**, 187 (1990).
11. Tsujikawa K., Tajima K., Ohashi M. *J. of Lightwave Technol.*, **18**, 1528 (2000).
12. Belov A.V., Guryanov A.N., Devyatykh G.G., Dianov E.M., Khopin V.F., Kurkov A.S., Mashinsky V.M., Miroshnichenko S.I., Neustruev V.B., Vechkanov N.N. *Sov. Lightwave Commun.*, **2**, 281 (1992).
13. Dianov E.M., Kurkov A.S., Mashinsky V.M., Neustruev V.B., Guryanov A.N., Devyatykh G.G., Khopin V.F., Miroshnichenko S.I., Vechkanov N.N. *OFC/IOOC'93 Tech. Dig.* (San Jose, California, 1993) TuL1, p. 51.
14. Guenot P., Nouchi P., Poumellec B. *OFC'99 Tech. Dig.* (San Diego, California, 1999) ThG2-1, p. 84.
15. Lines M.E., Reed W.A., Di Giovanni D.J., Hamblin J.R. *Electron. Lett.*, **35**, 1009 (1999).
16. Mashinsky V.M., Dianov E.M., Neustruev V.B., Lavrishchev S.V., Guryanov A.N., Khopin V.F., Vechkanov N.N., Sazhin O.D. *Proc. SPIE Int. Soc. Opt. Eng.*, **2290**, 105 (1994).
17. Ainslie B.J., Beales K.J., Cooper D.M., Day C.R. *Proc. SPIE Int. Soc. Opt. Eng.*, **425**, 15 (1983).
18. Abramov A.A., Bubnov M.M., Dianov E.M., Kol'chenko L.A., Semjonov S.L., Shchebunjaev A.G., Gurjanov A.N., Khopin V.F. *Electron. Lett.*, **29**, 1977 (1993).
19. Shibata N., Kawachi M., Edahiro T. *The Transactions of the IECE of Japan*, **E63**, 837 (1980).
20. Fermann M.E., Poole S.B., Payne D.N., Martinez F. *J. of Lightwave Technol.*, **6**, 545 (1988).
21. Hartog A.H., Gold M.P. *J. of Lightwave Technol.*, **LT-2**, 76 (1984).
22. Pinnow D.A., Rich T.C., Ostermayer F.W. Jr., DiDomenico M. Jr. *Appl. Phys. Lett.*, **22**, 527 (1973).
23. Ohashi M., Shiraki K., Tajima K. *J. of Lightwave Technol.*, **10**, 539 (1992).
24. Guenot P.L., Nouchi P., Poumellec B., Mercereau O. *Proc. Intern. Wire & Cable Symposium* (Eatontown, New Jersey, 1996) p. 679.
25. Rawson E.G. *Appl. Opt.*, **11**, 2477 (1972).
26. Marcuse D. *Appl. Opt.*, **14**, 3021 (1975).
27. Rawson E.G. *Appl. Opt.*, **13**, 2370 (1974).

Nobel Prize laureats walking about Göteborg (Sweden) during the International Conference on Atomic Physics, 1982. From left to right: A. Schawlow (USA), K. Zigben (Sweden), A.M. Prokhorov (USSR), I. Rabi (USA), N. Bloembergen (USA).